Telecommun Syst
DOI 10.1007/s11235-008-9103-3

Markov chain model for performance analysis of transmitter power control in contention based wireless MAC protocol

Muhammad Tahir · Sudip K. Mazumder

Abstract We have developed a three-state discrete-time Markov-chain model for the performance evaluation of contention-based medium access control (MAC) protocol. The proposed Markov-chain model is then used to analyze the carrier sense multiple access (CSMA) type MAC protocol for its delay and throughput characteristics with and without transmitter power control. Using simulations, the conditional capture probability (p_{cap}), which gives a measure of the effectiveness of transmitter power control due to the capture effect, is quantified and experiments are performed to validate these simulated data for the p_{cap}. To analyze the effect of transmitter power variation, the Markov-chain model is modified by incorporating the p_{cap}. Numerical results show significant throughput as well as delay performance improvement using transmitter power control.

Keywords Markov chain · Probability of capture · Access protocol · Distributed wireless control

1 Introduction

In a distributed control system [1, 2] (e.g. interactive power networks (IPNs) [3, 4], distributed generation, microgrids etc.) information among the nodes needs to be exchanged over a communication network to achieve stable operation while meeting performance bounds. We consider wireless communication networks for information exchange to achieve these control objectives for IPNs. Control systems require the data to be accurate, timely and lossless. But, a wireless-network is susceptible to random delays owing to interference and collisions due to multiple simultaneous transmissions (in case of random access) and channel nonlinearities. These delays degrade the system performance and in some cases can lead to instabilities [2]. An IPN node, due to the *continuous* availability of finite energy for wireless transceivers, offers the possibility of transmitter power control [due to the medium access control (MAC) protocol], thereby offering an effective mechanism for delay reduction and improvement in the network control performance.

In this paper we consider *collision-resolution* capability owing to transmitter power control, which is possible due to *capture effect* [5] i.e., the receiver is captured when, in case of collision due to multiple transmissions, a packet can be received successfully if its power is higher than the power of interfering packets by a certain threshold. The performance requirements of wireless networks for IPNs differentiate them from conventional wireless data communication networks. Below are some unique characteristics that differentiate the needs of a wireless network for distributed control of IPNs from a conventional wireless data network:

1. *Packet data size*: The data exchanged among the nodes in an IPN consisting of controller parameters, fault messages or protocol control packets is on the order of few bytes and is relatively much smaller compared to the data size in conventional wireless networks (e.g. IEEE 802.11). The data arrives randomly at different nodes and a contention based MAC protocol is a suitable choice for

M. Tahir
Department of Electrical and Computer Engineering, University of Illinois at Chicago, 851 S. Morgan Street, M/C 154, 1020 SEO, Chicago, IL 60607, USA
e-mail: mtahir1@uic.edu

S.K. Mazumder (✉)
Laboratory for Energy and Switching-Electronics Systems, Department of Electrical and Computer Engineering, University of Illinois at Chicago, 851 S. Morgan Street, M/C 154, 1020 SEO, Chicago, IL 60607, USA
e-mail: mazumder@ece.uic.edu

timely transmission to minimize delays under medium traffic. Small data size packets carrying system state variables are also exchanged randomly when the distributed control is implemented using estimation and need-based communication [6];

2. *MAC protocol*: Among the different contention based random access protocols ALOHA and CSMA-type protocols are leading contenders. It is well known that the throughput performance of a CSMA-type protocol is better than ALOHA under nominal conditions [7]. Due to the random access nature of the MAC protocol, collisions are unavoidable. CSMA/CA (a variant of CSMA using collision avoidance mechanism) employed in IEEE 802.11 is not a suitable choice in case of IPN. This is because, in CSMA/CA, the request-to-send (RTS) and clear-to-send (CTS) packets exchanged before actual data transmissions are about of the same size as that of the actual data packets in an IPN, which results in large overhead. In addition the associated large delays make the use of RTS and CTS packets impracticable. We consider slotted non-persistent CSMA (SNP-CSMA) MAC protocol [7] for data transfers in an IPN.

To better utilize the above mentioned distinguishing features we have. To capture the protocol dynamics for varying packet length and number of nodes, multiple transmitter power levels and dynamic channel conditions, we have designed a Markov-chain based MAC protocol (CSMA-type) model. The model is flexible and can be modified for other types of contention based MAC protocols.

In Sect. 2, we provide an overview of the work related to the theme of the present paper. Section 3 outlines a three-state Markov-chain model for the performance analysis of the system, which can accommodate variability in packet size and number of nodes. Subsequently, this Markov-chain model is used to assess the MAC protocol performance with and without transmitter power control. In Sect. 4, using simulation and experiments, we measure probability of a successful reception when there is a collision. This *conditional-capture probability* is denoted by $p(cap \mid coll)$ and will be abbreviated as p_{cap} here after. To enhance the effectiveness of capture phenomenon and as a result to maximize p_{cap}, we consider transmitter power control and show that it improves the system protocol delay and throughput performance significantly. Finally, we provide results for system-throughput and delay performances using the Markov-chain model.

2 Related work

Markov models have been widely used at the physical layer to model wireless communication channels, from the early work of Gilbert [8] to more recent papers studying their applicability to fading channels [9–13]. In particular finite-state Markov chains have been used to approximate both mathematical and experimental wireless medium fading models, including indoor channels [12], Rayleigh fading channels [13], and Ricean fading channels [14]. Markov modeling a the MAC layer is mainly used to model different types of back-off mechanism in contention based MAC protocols [15–17]. In [15, 16] binary exponential back-off mechanism is modeled using a two dimensional Markov-chain for the IEEE 802.11b MAC protocol. While in [17], a linear back-off mechanism is considered for the case of infrared communication based wireless MAC protocol. The authors in [18] have proposed Markov-based stochastic chains to model the 802.11b MAC-to-MAC channel behavior for both bit errors and packet losses. At least 9th order Markov chain is required to model the bit error process and is limited by the exponential complexity of the model. A generalized slotted-Aloha MAC protocol employing a two-state process at each node is proposed in [19], where the authors have used a Markov model for the generalized two-state Aloha protocol for throughput performance evaluation. An out of band signaling scheme is proposed in [20] to improve the throughput performance for high speed wireless LANs. The main idea is the adoption of two separate physical carriers: one devised to manage the channel access contention, and another to deliver information data. The authors in [21] have extended the model in [15] and characterize the channel activities governed by IEEE 802.11 DCF in multi-hop wireless networks from the perspective of an individual sender. In particular, the effect of PHY/MAC attributes (such as transmit power and physical carrier sense) in multi-hop wireless networks is considered, and analytical expression for the throughput attained by each sender is derived.

The transmitter power control is widely used for battery-life optimization as well as range and topology control. In [22] the authors have focused on MAC protocols, which control the transmission power level to minimize energy consumption while the transmitter power adjustments for topology control are discussed in [23]. A distributed algorithm for maximizing 1-hop broadcast coverage in dense wireless sensor networks using network density and node sending rate is provide in [24]. The algorithm allows each node to set the maximizing radio range using only local information and message eavesdropping without requiring extra protocol overhead. In contrast to the power control in [24] where power is increased to maximize the radio range, a power efficient MAC layer algorithm is proposed in [25] using minimum required power level for the transmission of data packets leading to an increase in the throughput. Unlike the algorithms in [24] and [25] where power levels are either maximized or minimized, we have used transmission power variation to resolve the collisions to increase the p_{cap} and as a result reduce the delay in successful packet transmission. Our approach is similar to the power ramping scheme

in [26] which is used to increase the transmission success rate for delayed preambles in mobile communications.

In a recent work [27], the authors have proposed a constant back-off window based scheme, which extends the model in [15] to investigate the performance of the IEEE 802.11 DCF multiple access scheme under general load conditions in single-hop configurations. The authors derive the size of the optimal constant window that maximizes the network throughput in saturation. This optimal constant window is used for all traffic loads and it is shown that the system operate quasi-optimally independent of the traffic load. In [28] an analytical model to compute the average service time experienced by a packet when transmitted in a saturated IEEE 802.11 ad hoc network is presented. When considering the delay performance in saturated random access networks using CSMA/CA based mechanism the authors in [28] emphasize that the binary exponential back-off algorithm appears inappropriate, and a large and constant contention window size is shown to be more efficient, with packet sizes being selected according to the network size. This is the basis for the constant back-off window assumption in our model. Unlike the Markov models in [15–17, 19] which are employed at each node, our proposed model [29] is for the complete network. The key advantage of our approach is reduced order network model as compared to node based modeling approaches. The proposed model is flexible and incorporates the effect of transmitter power variations using the idea of capture probability.

3 The Markov model

We develop a framework to analyze the delay and throughput performance using discrete-time Markov-chain model. The traffic generated in a distributed control system is mainly due to the exchange of state variables of the system. The number of state variables exchanged and their bit resolution can vary for different nodes. Therefore we model the packet length L as a discrete random variable uniformly distributed between a minimum (L_{min}) and a maximum (L_{max}) packet size. Time is slotted and packet length is an integer multiple of the slot time normalized to 1. It is assumed that, the slot time is equal to the channel propagation time (T_{prop}). The $W_{min}(= 1 + L_{min})$ and $W_{max}(= 1 + L_{max})$, correspond to the durations of the minimum and maximum collisions, respectively. The factor of '1' accounts for propagation delay (T_{prop}) because the channel becomes idle at the transmitting node, but is sensed busy by some other nodes until the end of next time slot. We assume a saturation model [15], where a node has data ready for transmission immediately after its successful transmission. This is possible in a control system where sampling can be performed at faster rate compared to the transmission rate.

When the nth node which is ready for transmission, senses the channel busy, it postpones the transmission by the back-off interval, which is a random variable sampled uniformly from the interval $(0, CW_n - 1)$, where CW_n is the maximum back-off window. Here we do not consider multiple back-off stages [15] due to the following reasons:

- The small packet data size in a control system along with multiple back-off stages will result in longer idle durations. It is also suggested in [28] that a large and constant contention window size is more efficient in contrast to the binary exponential back-off algorithm when considering the delay performance in saturated random access networks. As we will note later the performance of nonlinear multiple back-off mechanism [15] in terms of average number of transmissions per packet is comparable to the performance improvement using the capture effect along with constant back-off window. In addition using the constant back-off window with capture effect leads to better delay performance compared to the multiple back-off stages. This is due to collision resolutions when constant back-off window with capture is used in contrast to the collision avoidance in case of multiple back-off stages;
- In a control system it is more practical to send newly generated real-time data as compared to the previously delayed data. The presence of multiple back-off stages will result in delaying the transmission of new data arrivals and can lead to system performance degradation.

Using the approximation that each transmission attempt is independent of the previous transmissions, the probability of packet transmission (η_n) [15] from the node n in a given time slot is obtained using

$$\eta_n = \frac{2}{CW_n + 1}. \tag{1}$$

3.1 State transition probabilities

For the SNP-CSMA protocol the channel can be in one of the three possible states: idle state (i), successful transmission state (s) and collision state (c). Figure 1 shows Markov-chain based state diagram. There is no state-transition from state s to c because once the channel is occupied by a successful transmission, all the other nodes ready for transmission will find the channel busy and will back-off.

The probability that only node n transmits in a given time slot is given by

$$\alpha_n = \eta_n \prod_{j=1, j\neq n}^{N} (1 - \eta_j) \tag{2a}$$

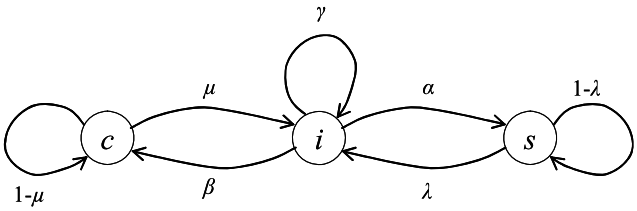

Fig. 1 Three state Markov-chain based state-transition diagram

where N is the total number of nodes in the network. The state-transition probability (α) corresponding to successful transmission, given by

$$\alpha = \sum_{n=1}^{N} \alpha_n, \tag{2b}$$

represents the probability that exactly one of the N nodes transmits in a given time slot. The probability that the channel is in state i and remains in state i implies that there is no transmission from any of the nodes and is given by

$$\gamma = \prod_{n=1}^{N} (1 - \eta_n). \tag{3}$$

The probability of collision due to two or more simultaneous transmissions is given by

$$\beta = 1 - \alpha - \gamma. \tag{4}$$

For the homogeneous network where the packet transmission probabilities are same at all the nodes, (i.e., $\eta_n = \eta$, $\forall n$), the transition probabilities for state i in (2b)–(4) can be combined, using binomial sum [30], as below

$$b_N(m, \eta) = \sum_{m=0}^{N} \frac{N!}{(N-m)!m!} \eta^m (1-\eta)^{N-m} \tag{5a}$$

where m $(0 \le m \le N)$ represents the number of simultaneous transmissions. When the network is in state i, the expression in (5a) can be written in terms of state-transition probabilities as

$$b_N(m, \eta) = \begin{cases} \gamma, & m = 0, \\ \alpha, & m = 1, \\ \beta, & 1 < m \le N. \end{cases} \tag{5b}$$

Once there is a transition from state i to state s or state c, all the new arrivals find the channel occupied and delay their transmission according to back-off algorithm. The state-transition probabilities μ and λ that are dependent on the packet length are obtained as follows:

$$\mu = \frac{1}{N} \sum_{n=1}^{N} \frac{1}{E[W_n]}, \qquad \lambda = \frac{1}{N} \sum_{n=1}^{N} \frac{1}{E[L_n]}. \tag{6}$$

In (6), $E[W_n]$ and $E[L_n]$ represent, respectively, the expected collision and packet lengths at node n and are expressed in number of slots.

3.2 Throughput and delay performance analysis

For the state diagram in Fig. 1 the transition probabilities are given by

$$\begin{aligned} P_i(k+1) &= \gamma P_i(k) + \mu P_c(k) + \lambda P_s(k), \\ P_c(k+1) &= \beta P_i(k) + (1-\mu) P_c(k), \\ P_s(k+1) &= \alpha P_i(k) + (1-\lambda) P_s(k), \end{aligned} \tag{7}$$

where a state-transition can occur only at the beginning of each slot. From the set of state equations in (7), the probability state-transition matrix (A) is given by

$$A = \begin{bmatrix} \gamma & \beta & \alpha \\ \mu & 1-\mu & 0 \\ \lambda & 0 & 1-\lambda \end{bmatrix}.$$

From the state diagram in Fig. 1, it is observed that the Markov-chain has one class and hence the steady-state or equilibrium probability vector exists [30]. The steady-state vector ($\vec{\pi}$) given by $\vec{\pi} = \lim_{x\to\infty} \vec{p}_0 A^x$ is the solution of $\vec{\pi} = \vec{\pi} A$, where $\vec{\pi} = [\pi^{(i)}\ \pi^{(c)}\ \pi^{(s)}]$ is independent of the initial state vector $\vec{p}_0$. The Markov-chain steady-state probabilities are used to characterize the system performance. System throughput (S) is the ratio of the time spent by the channel in the successful transmission state s (which is equivalent to the steady-state probability $\pi^{(s)}$) to the total time and is given by

$$S = \frac{\pi^{(s)}}{\sum_{j:j\in\{i,s,c\}} \pi^{(j)}}. \tag{8}$$

Using the fact that $\sum_{j:j\in\{i,s,c\}} \pi^{(j)} = 1$, we have $S = \pi^{(s)}$. Solving for the steady-state successful transmission probability $\pi^{(s)}$, the throughput equation in (8) can be written only in terms of state-transition probabilities given by

$$S = \frac{\alpha}{(1+\lambda/\alpha)[(1-\gamma)-\beta] + \beta(\lambda/\mu)}. \tag{9}$$

To analyze the delay performance we first calculate the offered traffic to the channel.

Definition Offered traffic G is defined as the expected length (in time slots) of the arriving packets at all the nodes per unit packet time and is given by

$$G = \sum_{n=1}^{N} \eta_n E[L_n]. \tag{10}$$

Table 1 Parameters used in simulation setup

Nominal network parameters	Values
Transmission rates	1.5 Mbps
Network radius	200 m
Average packet length $E[L]$	40 bits
Capture threshold (ρ)	6 dB
Power loss exponent (υ)	3
Standard deviation for shadow fading (σ)	6 dB
Transmission power	3–19 dBm

But the actual transmission traffic G' is the fraction of the offered traffic in (10), which finds the channel in idle state and is given by $G' = G\pi_i$. Now using similar arguments as in [7] we calculate the average packet delay (D) experienced by a node as follows:

$$D = (G/S - 1)\psi + G'/S(T_{trans} + T_{prop}), \tag{11}$$

where T_{trans} is the packet transmission time and ψ is the average time for each retransmission obtained by scaling with the slot duration and is given by

$$\psi = \frac{1}{N}\sum_{n=1}^{N}\left(\frac{CW_n}{2E[L_n]}\right)T_{trans}.$$

3.3 Model validation

To validate the proposed model, we performed simulations using the Matlab program that emulates the protocol model and traffic arrivals under saturation throughput conditions closely. In particular after each successful packet transmission from a node, a new packet is generated immediately; subsequently the node backs off for a random interval sampled from CW_n. The values of the parameters used to obtain the results are summarized in Table 1.

We have used a fixed packet length of 40 bits for the simulations. Figure 2 shows that the Markov model is very accurate: numerical results for the network throughput (shown as solid lines) practically coincide with the simulation results (shown by symbols) for different number of nodes in the network. One key observation is that, a small variation in η at maximum throughput results in fast degradation in the system throughput performance for large number of nodes.

4 Modified Markov model

In the sequel we describe how the Markov model can be modified to take into account the effect of transmitter power control. For that we define probability of capture below and later use it as a performance measure of the transmitter power control.

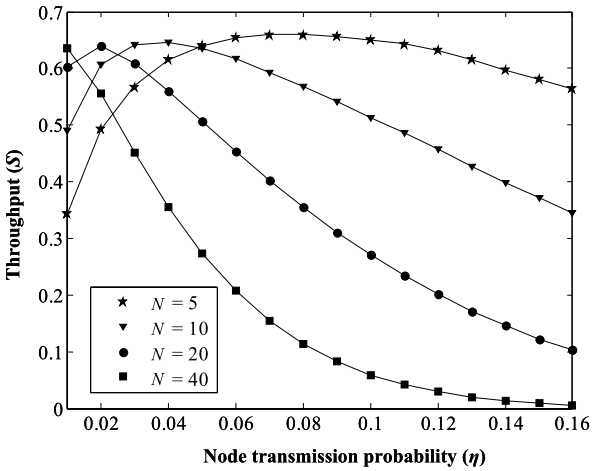

Fig. 2 Effect of number of nodes on the system throughput performance as a function of packet-transmission probability from a node. For these results $E[L] = 40$ bits is used

4.1 Probability of capture (p_{cap})

To analyze the effect of transmitter power variation on p_{cap} we use the wireless channel incorporating the effect of path loss, shadowing and multi-path fading. The effect of propagation through the channel is multiplicative and the received power Γ_R is obtained by multiplying the transmitted power Γ_T with random variables due to path loss, multi-path fading and shadowing [31]:

$$\Gamma_R = R^2 K e^{\xi} r^{\upsilon} \Gamma_T. \tag{12}$$

In (12), R has Rayleigh or Ricean distribution to account for multipath, ξ is Gaussian distributed random variable with zero mean and standard deviation σ (dB), $K = e^{\sigma^2/2}$and Ke^{ξ} represents the effect of shadowing, υ is the power loss exponent that varies between 2 to 6 depending on the characteristics of the environment [32] and r is the distance between the transmitter and receiver pair and is uniformly distributed in a unit circle. In case of collision due to k simultaneous transmissions, there will be power capture at the receiver if the power received at the receiver due to transmitter j satisfies the relationship given by

$$\Gamma_{Rj} \geq \rho\left(\sum_{l=2, l\neq j}^{k} \Gamma_{Rl} + \mathrm{Z}\right), \quad k = 2, 3, \ldots, N, \tag{13}$$

where Z is the additive noise that is independent of the transmitter power levels and ρ is the capture threshold that determines the minimum carrier to interference ratio required for a successful reception and is determined mainly by the type of modulation and receiver sensitivity. The typical value for the threshold factor for the narrowband systems lies within 3–10 dB. The probability of a successful capture [33] at the

receiver for the transmission from node j, when there is a collision among k transmitting nodes, is given by

$$p_j(cap \mid k) = \Pr\left(\Gamma_{Rj} \geq \rho\left(\sum_{l=2, l\neq j}^{k} \Gamma_{Rl} + Z\right)\right). \quad (14)$$

But there are k different nodes participating in the collision and any of these nodes can capture the receiver with equal probability. The resulting capture probability $p(cap \mid k)$, when there is collision due to k simultaneous transmissions, is given by

$$p(cap \mid k) = kp_j(cap \mid k), \quad k = \{2, 3, \ldots, N\}. \quad (15)$$

It is important to notice that $p_{cap} \equiv (p(cap \mid \text{all } k))$ is the overall capture probability that accounts for all the successful captures when there is a collision due to any number of simultaneous transmissions, while $p(cap \mid k)$ is the probability of a successful capture when there is collision due to exactly k simultaneous transmissions.

4.2 Modified Markov state diagram

We incorporate the effect of p_{cap} and redraw the Markov state diagram shown in Fig. 3. In the presence of capture effect and transmitter power control some of the collisions are resolved and the state-transition probability from state i to state s is increased while from state i to state c is reduced by βp_{cap}. The modified state-transition matrix is given by

$$A' = \begin{bmatrix} \gamma & \beta(1-p_{cap}) & \alpha+\beta p_{cap} \\ \mu & 1-\mu & 0 \\ \lambda & 0 & 1-\lambda \end{bmatrix}.$$

The corresponding delay equation becomes

$$D_{cap} = (G/S_{cap} - 1)\psi + G'/S_{cap}(T_{trans} + T_{prop}) \quad (16)$$

where S_{cap}, the throughput in the presence of capture, is given by

$$S_{cap} = \frac{(\alpha+\beta p_{cap})}{[(1+\lambda/(\alpha+\beta p_{cap}))][1-\gamma-\beta(1-p_{cap})] + \beta(1-p_{cap})(\lambda/\mu)}. \quad (17)$$

The expression for S_{cap} is obtained by solving $\vec{\pi}_{cap} = \vec{\pi}_{cap}A'$ for $\pi_{cap}^{(s)}$ where $\vec{\pi}_{cap} = [\pi_{cap}^{(i)}\ \pi_{cap}^{(c)}\ \pi_{cap}^{(s)}]$.

5 System performance

5.1 Probability of capture measurement

To analyze the effect of transmitter power on p_{cap} we have done simulations using the channel model described in Sect. 4.1. The mean packet length $E[L]$ can be represented in bits by multiplying the packet length in slots by bits per slot. For the simulations we have used packet length of 40 bits for all the nodes. The parameters used in the simulations are tabulated in Table 1.

In Fig. 6(a) the effect of transmitter power variation on $p(cap \mid k = 2)$, $p(cap \mid k = 3)$, $p(cap \mid k = 4)$ and p_{cap} is shown. The results show that $p(cap \mid k = 2)$ is the main component that contributes to p_{cap}. As the number of nodes (k) participating in a collision increase the corresponding capture probability decreases and is shown in Fig. 6(a) for the case $k = \{2, 3, 4\}$. It is important to realize that the probability of collision due to k simultaneous transmissions is a decreasing function for increasing values of k. Hence main component that contributes to p_{cap} is $p(cap \mid k = 2)$.

To verify our simulation results we conducted experiments in the indoor laboratory conditions to measure p_{cap}. The hardware setup used to conduct the experiments as shown in Fig. 4 is based on a two chip solution (ML2722 and ML2751) from Micro Linear [34, 35] with maximum data rate of 1.5 Mbps and 12 selectable frequency channels each of 2.048 MHz band-width. The maximum transmitter power is 21 dBm and the receiver sensitivity is −95 dBm. The base-band processing is done using field-programmable gate array (FPGA) and the digital signal processor (DSP). Figure 4 shows the block diagram of the wireless communication hardware and its interface with the FPGA and DSP.

The digital wireless interface uses frequency-shift keying (FSK) modulation and operates in unlicensed 902–928 MHz ISM band. To measure p_{cap} it is required that all the packets transmitted from different nodes encounter collisions. This is achieved easily by continuous transmission of packets from each of the transmitters. As a result all the suc-

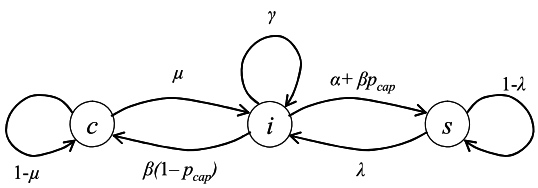

Fig. 3 Modified Markov-chain state diagram to incorporate the effect of transmitter power control using p_{cap}

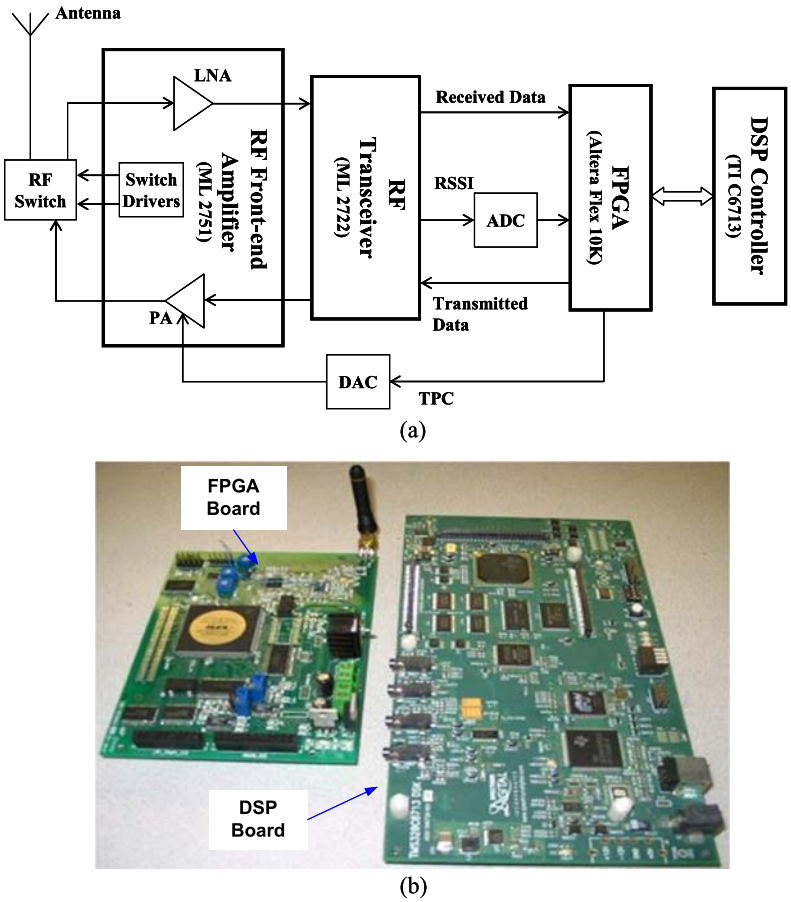

Fig. 4 The hardware testbed used for measurements and its equivalent block diagram. The received signal strength indicator (RSSI) is used to receive only those data for which the signal strength is larger than a minimum value. In the block diagram, TPC is transmitter power control, LNA is low noise amplifier, PA is power amplifier, ADC is analog to digital converter and DAC is digital to analog converter

cessful receptions are due to the capture phenomenon. We perform the experiment for three cases: (a) collision due to two simultaneous transmissions, (b) collision due to three simultaneous transmissions and (c) collision due to four simultaneous transmissions. In all the measurement scenarios of Fig. 5 the minimum separation between the transmitter and receiver is large enough that the measurements fall in the *Far-Field region*. The Far-Field region is defined as the region at a minimum distance F from the transmitting antenna given by $F = \Delta^2/(4\Theta)$ [36], where Δ is the radius of the sphere with the largest dimension of the antenna and Θ is the wavelength corresponding to the frequency of operation.

Figure 5(a) shows the spatial arrangement for the nodes when packet collisions are due to two simultaneous transmissions. In case of three and four transmitting nodes the arrangements are as shown in Fig. 5(b) and (c), respectively. The distances among different pairs of nodes used in the measurements are given in the accompanying table shown in Fig. 5(d). In the experimental measurements we vary the transmitter power at all the transmitting nodes except Node 2. The power at Node 2 is kept fixed at the maximum transmit level of 19 dBm. A total of 2×10^6 packets of length 40 bits are successfully received due to capture and the receiver stops after receiving these many packets. The receiver also records the timer value and the number of timer ticks (timer was running at 1 msec) for measuring the time elapsed between first and last reception. The total number of packets received due to successful capture from the k nodes and the time elapsed in reception are used to calculate $p(cap \mid k)$. The measured value is based on the fact that the collision probability is one. Given there is a collision for each transmission $p(cap \mid k)$ is obtained using

$$p(cap \mid k) = \frac{\text{number of packets successfully received per unit time for collision among } k \text{ packets}}{\text{total number of packets transmitted per node per unit time}}.$$

For the collision due to two simultaneous transmissions, the transmitting nodes are at same distance from the receiver, and for the same transmit power $p(cap \mid k = 2)$ is low. As the transmit power level is reduced at Node 1 $p(cap \mid k = 2)$ starts increasing. The value of $p(cap \mid k = 2)$ is higher than 0.7 when the difference between the power levels of the two transmitters is 13 dB as shown in Fig. 6(b). For three transmitting nodes the arrangement is shown in Fig. 5(b). In this case all three transmitting nodes transmit packets continuously without any empty time slots to ensure that there is always a collision due to three simultaneous transmissions. Due to the transmitter power variation at Node 1 and Node 4 a large number of combinations for transmitting power levels are possible and we follow the steps outlined below to measure $p(cap \mid k = 3)$:

- *Step 1*: Vary the transmit power at Node 1 while the other two transmitting nodes (Node 2 and Node 4) continue to transmit at their assigned power levels (starting at maximum power of 19 dBm);
- *Step 2*: Decrement the transmit power at Node 4 while keeping the power at Node 2 fixed (at 19 dBm) and repeat Step 1 till transmit power at Node 4 is 3 dBm.

The value for $p(cap \mid k = 3)$ is obtained by taking the average for the power variation at Node 4 and is shown in Fig. 6(b) as a function of transmitter power variation at Node 1. Similar procedure is adopted for the measurement of $p(cap \mid k = 4)$, where averaging is done for the power variation at Node 4 and Node 5. It is difficult to measure $p(cap \mid k)$ for higher values of k due to a large number of possible combinations of transmitter power levels. Comparing the experimental measurement results for $k = \{2, 3, 4\}$ with the simulations we conclude that p_{cap} will be close to $p(cap \mid k = 2)$.

The simulation and experimental results for p_{cap} are close. The reason for getting slightly higher value of p_{cap} experimentally is that the capture model used in the simulations is pessimistic. In the simulations for successful capture it requires that the power from one of the nodes should be larger than the sum of the powers from all other interfering

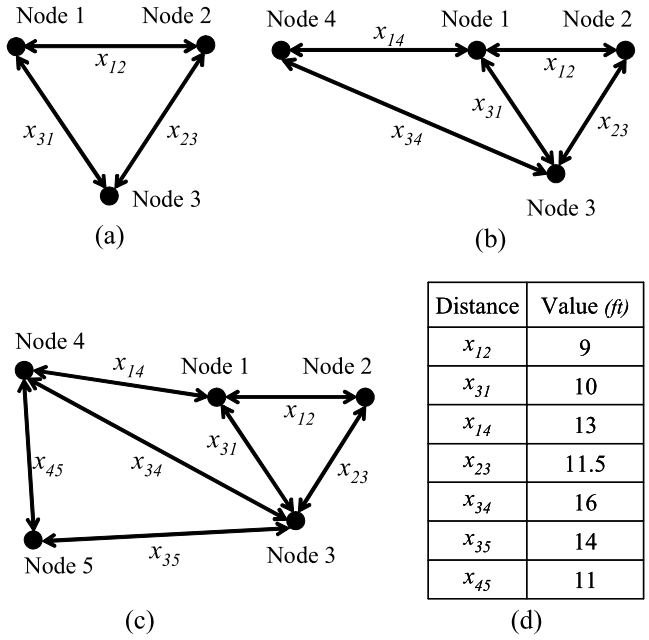

Distance	Value *(ft)*
x_{12}	9
x_{31}	10
x_{14}	13
x_{23}	11.5
x_{34}	16
x_{35}	14
x_{45}	11

(d)

Fig. 5 The arrangement for (**a**) two transmitting nodes, (**b**) three transmitting nodes and (**c**) four transmitting nodes. (**d**) Distance between different pairs of nodes. The diagrams are not drawn to the scale. In all arrangements Node 3 is receiving node

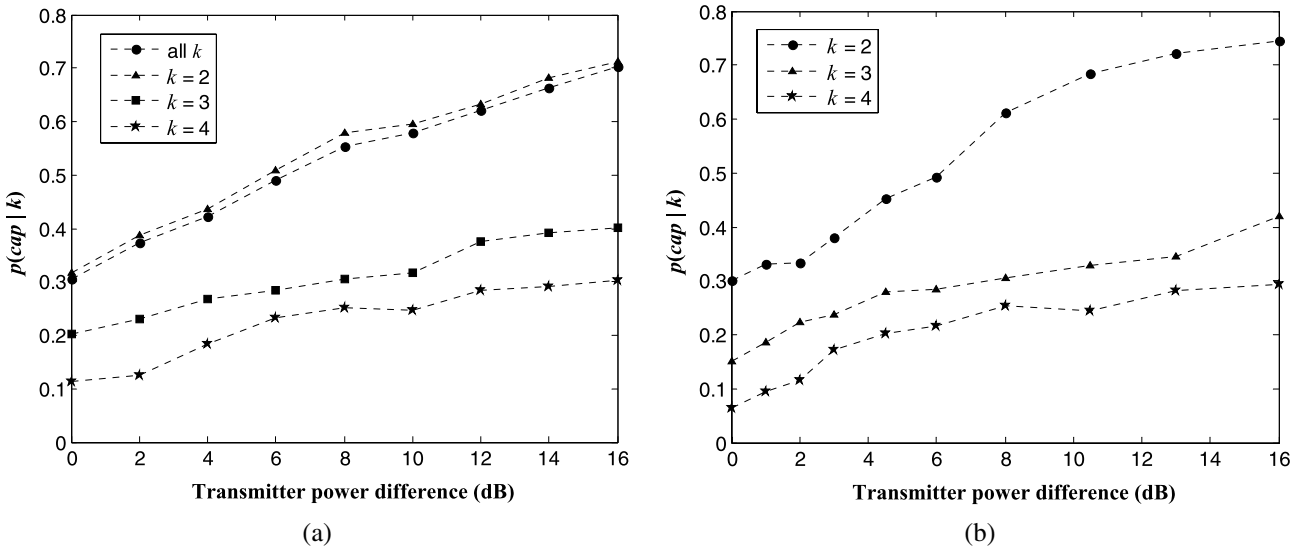

Fig. 6 $p(cap \mid k)$ for different number of transmitting nodes as a function of transmitter power variation. (**a**) Simulation and (**b**) experimental results using the platform in Fig. 4

nodes by the threshold. In practice it is quite possible that the signals from two of the interfering nodes experience destructive interference and a successful capture occurs even if the power of the strongest signal is not larger than the sum of the powers from the interfering nodes.

5.2 Performance evaluation

Numerical results are presented to evaluate the system performance using our Markov-chain model. First we observe how the steady state probabilities are affected by varying the number of nodes in the network with and without capture. Then we analyze the effect of back-off window size on the system throughput and the channel idle time. Later we have used the modified Markov model to see the effectiveness of capture phenomenon on the system throughput, average packet delay and average number of transmissions per packet.

The steady state probabilities given by $\vec{\pi}$ and $\vec{\pi}_{cap}$ as a function of number of nodes are shown in Fig. 7(a) and (b) respectively. As expected the capture phenomenon does not affect the idle state probability. It improves the throughput performance by resolving some of the packet collisions. Figure 8 shows the effect of the maximum back-off window size ($CW_n = CW,\ \forall n$) variation on the throughput performance of the network as a function of number of nodes. As can be seen the optimal value of CW depends on the number of contending nodes in the network. For example, a high value of CW (e.g. 256 in this case) gives excellent throughput performance in case of 40 contending nodes.

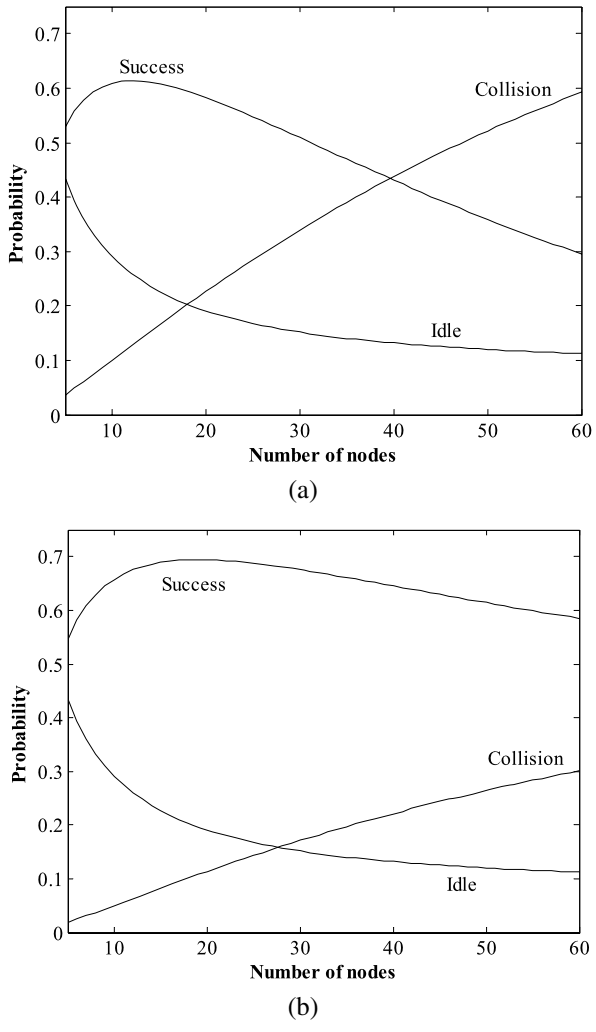

Fig. 7 Steady state probabilities for the three states (success (s), collision (c), idle (i)) of the network: (**a**) without capture ($\vec{\pi}$) and (**b**) with capture ($\vec{\pi}_{cap}$) for $p_{cap} = 0.5$

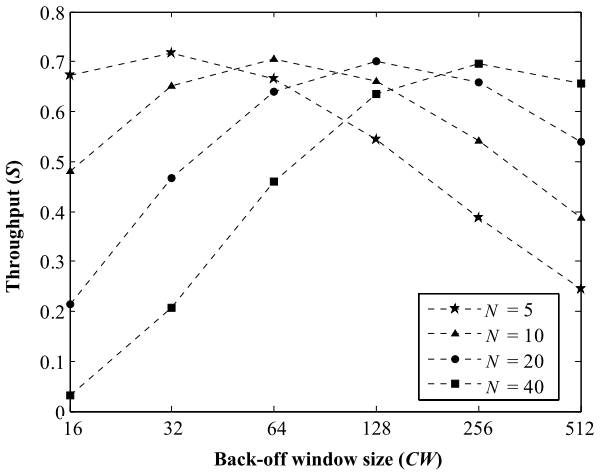

Fig. 8 Effect of back-off window size on the system performance. For these results $E[L] = 40$ bits is used

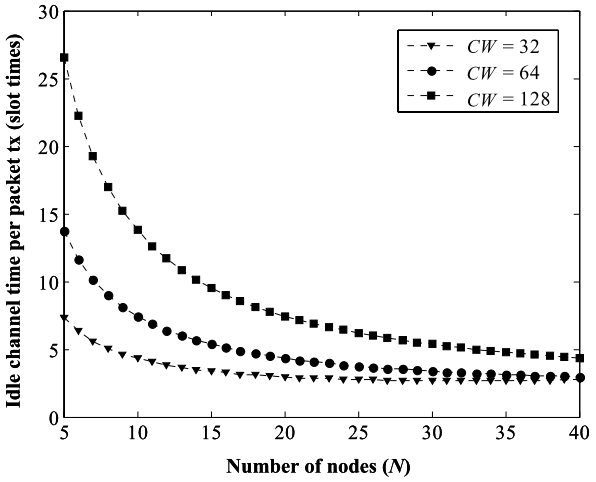

Fig. 9 Average number of channel idle time slots per successful packet transmission. $E[L] = 40$ bits is used

The average number of channel idle slots per packet transmission time i.e. $(\pi^{(i)}E[L]/\pi^{(s)})$ versus the number of nodes in the network is plotted in Fig. 9 for three different values of contention window CW. We observe that in general the number of idle slots per packet transmission is high due to small packet lengths. The effect is more pronounced in case of larger CW when the number of nodes in the network is small and adaptive window size selection is required depending on the number of nodes in the network. The effect of p_{cap} on the system throughput performance is shown in Fig. 10. For the performance evaluation $p_{cap} = 0.7$, being the lower between the simulation and the experimental results, is chosen. This gives a minimum performance gain attained when the transmitter power difference is 16 dB. At $p_{cap} = 0.7$ there is a considerable performance gain near the maximum throughput point. But as the offered traffic G given by (10) is further increased beyond the maximum throughput point the effect of capture probability becomes more dominant due to the increased number of collisions and maintains a throughput close to its saturation value for $p_{cap} = 0.7$. The value of $p_{cap} = 0.3$ correspond to a 0 dB transmitter power difference as shown in Fig. 6(a) and (b). Figure 11 compares the system delay performance for different values of capture probability. For an offered traffic $G = 20$ the delay becomes approximately half for capture probability of 0.7 compared to 0.3 (0 dB transmitter power difference).

Another measure of interest is the average number of transmissions per packets and can be obtained using the state transition probabilities. We define *collision probability* for node n $(p_{coll}(n))$ to be the probability that a trans-

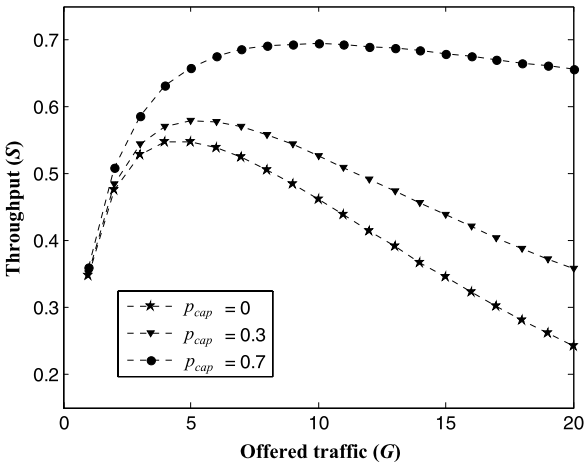

Fig. 10 Throughput performance for different capture probabilities for $N = 10$ and $E[L] = 40$ bits. The p_{cap} values correspond to the power level difference at the transmitters

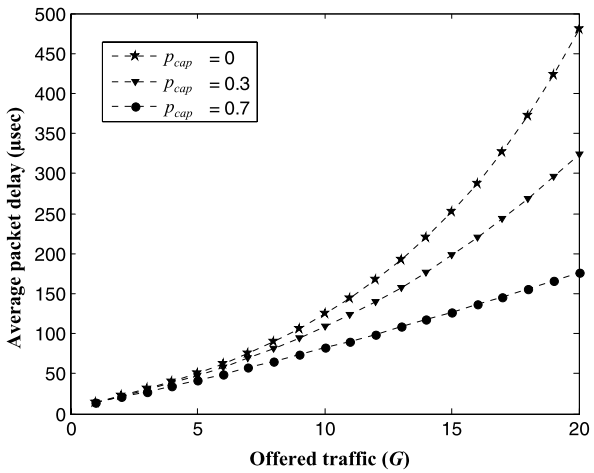

Fig. 11 System delay performance for different capture probabilities for $N = 10$ and $E[L] = 40$ bits

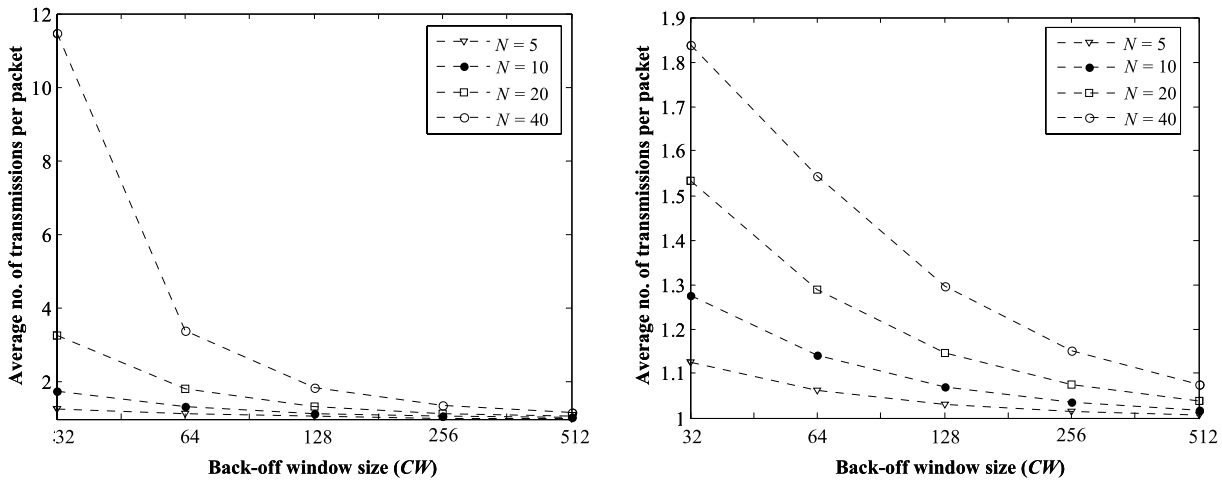

Fig. 12 Average number of transmissions per packet: (**a**) without capture and (**b**) with capture for $p_{cap} = 0.5$

mission from node n in a time slot will collide with any other transmission in the same time slot and is $p_{coll}(n) = 1 - \alpha_n - \gamma$. Using (2a) and (3) this simplifies to $p_{coll}(n) = 1 - (1-\eta)^{(N-1)}$. Using the assumption that each node transmits independent of the transmissions from other nodes, the average number of transmissions per packet without capture is given by $1/(1 - p_{coll}(n))$. The average number of transmissions per packet can be quite high for larger number of nodes in the network when the capture effect is not considered as shown in Fig. 12(a). When the effect of the capture is considered the expression for average number of transmissions becomes $1/(1 - p_{coll}(n)(1 - p_{cap}))$. There is a significant performance improvement in terms of average number of transmissions per packet with capture effect as shown in Fig. 12(b). The average number of packet transmissions per packet with multiple back-off stages is studied in [15] for IEEE 802.11 with the number of back-off stages equal to 6. The performance of nonlinear multiple back-off mechanism [15] in terms of average number of transmissions per packet is comparable to the performance improvement shown in Fig. 12(b) using capture effect. In addition the constant window with capture effect approach leads to better delay performance compared to the multiple back-off stages. This is due to the collision resolution when constant window with capture is used in contrast to the collision avoidance when multiple back-off stages are used.

6 Conclusions

The idea of wireless transmitter power control is applied to interactive power networks (IPNs) to minimize the delays due to contention based medium access control (MAC) protocol. The effectiveness of the transmitter power control depends on the receiver sensitivity and the size of the network in terms of coverage area. From the results it is observed that the improvement in the performance due to transmitter power control scheme increases with increasing network traffic. The performance gain for larger network size is bound by an upper limit on the transmitter power due to the regulations as most of the networks operate in license-free bands.

The Markov-chain model (described in this paper) evaluates the MAC protocol performance in the presence of capture probability and can be used for other contention-based MAC protocols by modifying the state-transition probabilities in Fig. 1. The model gives the average system performance parameter values and is capable of incorporating heterogeneous traffic patterns from the nodes.

As a future work, we plan to investigate the effect of increase in the number of power levels versus the increase in the separation between two power levels. To minimize the delay further and allow the coexistence of multiple transmissions, a physical layer based on code-division multiple access (CDMA) [37] or orthogonal frequency-division multiplexing (OFDM) [37] can be a good option. When the wireless network is multi-hop, joint design of routing protocols along with MAC protocols may be required.

Acknowledgements This work is supported by the National Science Foundation (NSF) CAREER Award (Award No. 0239131) and Office of Naval Research (ONR) Young Investigator Award (Award No. N000140510594) received by Prof. Mazumder in the years 2003 and 2005, respectively. However, any opinions, findings, conclusions, or recommendations expressed herein are those of the authors and do not necessarily reflect the views of the NSF and ONR. The authors are thankful to Professor Charles Tier, Department of Mathematics, University of Illinois at Chicago, for useful discussions on the Markov-chain based model.

References

1. Zhang, W. (2003). Stabilization of networked control systems over a sharing link using ALOHA. *Proceedings of IEEE Conference on Decision and Control*, *1*, 204–209.
2. Zhang, W., Branicky, M. S., & Phillips, S. M. (2001). Stability of networked control systems. *IEEE Control System Magazine*, *21*(1), 84–99.
3. Mazumder, S. K., Acharya, K., & Tahir, M. (2005). Wireless control of spatially distributed power electronics. *Proceedings of IEEE Applied Power Electronics Conference*, *1*, 75–81.
4. Acharya, K., Tahir, M., & Mazumder, S. K. (2006). Communication fault-tolerant wireless network control of a load-sharing multiphase interactive power network. In *Proceedings of IEEE power electronics specialist conference* (pp. 1167–1174).
5. Kim, J. H., & Lee, J. K. (1999). Capture effects of wireless CSMA/CA protocols in Rayleigh and shadow fading channels. *IEEE Transactions on Vehicular Technology*, *48*(4), 1277–1286.
6. Xu, Y., & Hespanha, J. P. (2004). Optimal communication logics in networked control systems. *Proceedings of IEEE Conference on Decision and Control*, *4*, 3527–3532.
7. Kleinrock, L., & Tobagi, F. (1975). Packet switching in radio channels: part I. Carrier sense multiple access modes and their throughput delay characteristics. *IEEE Transactions on Communications*, *23*(12), 1400–1416.
8. Gilbert, E. N. (1960). Capacity of a burst-noise channel. *Bell System Technical Journal*, *39*, 1253–1266.
9. Zorzi, M., Rao, R. R., & Milstein, L. B. (1995). On the accuracy of a first-order Markov model for data block transmission on fading channels. In *Proceedings of IEEE ICUPC* (pp. 211–215).
10. Turin, W., & Van Nobelen, R. (1998). Hidden Markov modeling of fading channels. In *Proceedings of VTC* (pp. 1234–1238).
11. Kim, Y. Y., & Li, S. Q. (1998). Modeling fast fading channel dynamics for packet data performance analysis. In *Proceedings of INFOCOM* (pp. 1292–1300).
12. Chen, A. M., & Rao, R. R. (1998). On tractable wireless channel models. In *Proceedings of international symp. on personal, indoor, and mobile radio comm.* (pp. 825–830).
13. Wang, H. S., & Moayeri, N. (1995). Finite-state Markov channel—a useful model for radio communication channels. *IEEE Transactions Vehicular Technology*, *44*(1), 163–171.
14. Pimentel, C., & Blake, I. F. (1998). Modeling burst channels using partitioned Fritchman's Markov models. *IEEE Transactions Vehicular Technology*, *47*(3), 885–899.
15. Bianchi, G. (2000). Performance analysis of the IEEE 802.11 distributed coordination function. *IEEE Journal on Selected Areas in Communications*, *18*(3), 535–547.

16. Bianchi, G. (1998). IEEE 802.11—Saturation throughput analysis. *IEEE Communications Letters*, *2*, 318–320.
17. Vitsas, V. (2003). Throughput analysis of linear backoff scheme in wireless LANs. *Electronics Letters, 39*(1).
18. Khayam, S. A., & Radha, H. (2003). Markov-based modeling of wireless local area networks. In *Proceedings of ACM mobicom international workshop on modeling, analysis and simulation of wireless and mobile systems* (pp. 100–107).
19. Richard, T. B. M., Misra, V., & Rubenstein, D. (2006). Modeling and analysis of generalized slotted Aloha MAC protocols in cooperative, competitive and adversarial environments. In *Proceedings of international conference on distributed computing systems* (p. 62).
20. Tantra, J. W., Foh, C. H., Tinnirello, I., & Bianchi, G. (2007). Out-of-band signaling scheme for high speed wireless LANs. *IEEE Transactions on Wireless Communications*, *6*(9), 3256–3267.
21. Yang, Y., Hou, J. C., & Kung, L.-C. (2007). Modeling the effect of transmit power and physical carrier sense in multi-hop wireless networks. In *Proceedings of INFOCOM* (pp. 2331–2335).
22. Chen, J.-C., Sivalingam, K. M., Agrawal, P., & Kishore, S. (1998). A comparison of MAC protocols for wireless local networks based on battery power consumption. *Proceedings of IEEE INFOCOM*, *1*, 150–157.
23. Ramanathan, R., & Hain, R. (2000). Topology control of multihop wireless networks using transmit power adjustment. *Proceedings of IEEE INFOCOM*, *2*, 404–413.
24. Li, X., Nguyen, T. D., & Martin, R. P. (2004). Using adaptive range control to maximize 1-hop broadcast coverage in dense wireless networks. In *Proceedings of SECON* (pp. 397–405).
25. Poon, E., & Li, B. (2003). Smartnode: Achieving 802.11 mac interoperability in power-efficient ad hoc networks with dynamic range adjustments. In *Proceedings of ICDCS* (pp. 650–657).
26. Yang, Y., & Yum, T.-S. P. (2005). Analysis of power ramping schemes for UTRA-FDD random access channel. *IEEE Transactions on Wireless Communications*, *4*(6), 2688–2693.
27. Anouar, H., & Bonnet, C. (2007). Optimal constant-window backoff scheme for IEEE 802.11 DCF in single-hop wireless networks under finite load conditions. *Springer Journal on Wireless Personal Communication*, *43*, 1583–1602.
28. Carvalho, M. M., & Garcia-Luna-Aceves, J. J. (2003). Delay analysis of IEEE 802.11 in single-hop networks. In *Proceedings of IEEE international conference on network protocols* (pp. 146–155).
29. Tahir, M., & Mazumder, S. K. (2007). Markov-chain-model-based performance analysis of transmitter power control in wireless MAC protocol: Towards delay minimization in power-network control. In *Proceedings of IEEE international conference on advanced information networking and applications* (pp. 909–916).
30. Karlin, S., & Taylor, H. E. (1975). *A first course in stochastic processes* (2nd ed.). California: Academic Press.
31. Hajek, B., Krishna, A., & LaMaire, R. O. (1997). On the capture probability for a large number of stations. *IEEE Transactions on Communications*, *45*(2), 254–260.
32. Parsons, J. D. (1992). *The mobile radio propagation channel*. New York: Wiley.
33. Zorzi, M., & Borgonovo, F. (1997). Performance of capture-division packet access with slow shadowing and power control. *IEEE Transactions on Vehicular Technology*, *46*(3), 687–696.
34. Micro Linear, ML2722. 900 MHz Low-IF 1.5 Mbps FSK Transceiver. http://www.microlinear.com/downloads/DS/DS2722-F-05.pdf.
35. Micro Linear, ML2751. Integrated Power Amplifier, LNA & Pin Diode Drivers. http://www.microlinear.com/downloads/DS/DS2751-F-03.pdf.
36. Saunders, S. R. (1999). *Antennas and propagation for wireless communication systems*. New York: Wiley.
37. Goldsmith, A. (2005). *Wireless communications*. New York: Cambridge University Press.

Muhammad Tahir received the B.Sc. degree in Electrical Engineering and the M.Sc. degree in Computer Engineering from the University of Engineering and Technology Lahore, Pakistan in 1999 and 2003 respectively. From 2000 to 2003 he served as lecturer in the Electrical Engineering Department, the University of Engineering and Technology Lahore. Since 2004 he is working towards his Ph.D. at the Laboratory for Energy and Switching-electronics Systems (LESES), Department of Electrical and Computer Engineering, University of Illinois, Chicago. His research interests include distributed optimization of wireless network resources for network control of high frequency switching systems and analysis of time delay systems. He is the coauthor of the IEEE AINA 2007 Outstanding Student Paper Award.

Sudip K. Mazumder is the Director of Laboratory for Energy and Switching-electronics Systems (LESES) and an Associate Professor in the Department of Electrical and Computer Engineering at the University of Illinois, Chicago. He has over 10 years of professional experience and has held R&D and design positions in leading industrial organizations. His current areas of interests are distributed control-communication interface for interactive power networks, alternate energy systems, photonically-triggered power semiconductor devices, and systems-on-chip/module.

Dr. Mazumder received the prestigious 2007 Faculty Research Award and the 2006 Diamond Award from the University of Illinois, Chicago for Outstanding Research performance. He received the ONR Young Investigator Award and NSF CAREER Award in 2005 and 2002, respectively, and the Prize Paper Award from the IEEE Transactions on Power Electronics in 2002. He is the Editor-in-Chief for International Journal of Power Management Electronics since 2006. He is an Associate Editor for the IEEE Transactions on Industrial Electronics since 2003 and was the Associate Editor for IEEE Power Electronics Letters till 2005. He also co-received the 2007 IEEE Outstanding Student Paper Award at the IEEE International Conference on Advanced Information Networking and Applications with his PhD student Muhammad Tahir.